Journal of Molecular Structure 1237 (2021) 130391

Contents lists available at ScienceDirect

Journal of Molecular Structure

journal homepage: www.elsevier.com/locate/molstr

A single-step multicomponent synthesis of a quinoline derivative and the characterization of its cyclodextrin inclusion complex

Luciana Matos Alves Pinto[a,b,*], Oluwatomide Adeoye[b], Sérgio Scherrer Thomasi[a], Ana Paula Francisco[b], Helena Cabral-Marques[b]

[a] Chemistry Department, Universidade Federal de Lavras, Campus Universitário s/n, C.P. 3037, 37200-900 Lavras/MG, Brazil
[b] Research Institute for Medicines (iMed.ULisboa), Faculty of Pharmacy, Universidade de Lisboa, Av. Prof. Gama Pinto, 1649-003 Lisbon, Portugal

ARTICLE INFO

Article history:
Received 22 February 2021
Revised 24 March 2021
Accepted 26 March 2021
Available online 6 April 2021

Keywords:
Cyclodextrin
Green chemistry
Hexahydroquinoline
Multicomponent synthesis
Single-step reaction

ABSTRACT

Multicomponent synthesis are convergent reactions in which three or more starting materials react in a single step to form the product. In the discovery and development of new drugs, multicomponent reactions offer several advantages over traditional synthesis: shorter experiment time, less need for laboratory techniques and scalability. Thus, the objective of this work was to perform the multicomponent synthesis of a hexahydroquinoline compound whose pharmacological activity has been described previously. The synthesis product was characterized by spectroscopic techniques such as Fourier transform infrared spectrometry and ^{1}H, ^{13}C and HMQC nuclear magnetic resonance (NMR). The mechanism of the reaction was proposed to include a conjugated Michael addition. Subsequently, inclusion complexes (ICs) at 1:1 and 1:2 stoichiometries were prepared with the appropriate cyclodextrin to increase the aqueous solubility and bioavailability of this molecule. Kneading and lyophilization (LYO) methods were used to prepare the inclusion complexes, which were evaluated by phase solubility and ^{1}H NMR spectroscopy, with LYO at a 1:2 stoichiometry having the best results. The ICs were then characterized by differential scanning calorimetry, near-infrared spectroscopy and *in vitro* dissolution tests, which verified a slower release of the compound with the potential to improve its biological properties.

1. Introduction

Some of the goals of green chemistry in the synthesis of active compounds are to minimize steps, save time and use nontoxic reagents. To achieve these goals, multicomponent synthesis (MS) allows us to obtain compounds from three or more reagents in a single step. Thus, the process can be executed in less time and with less need for purification [1]. The main goal of this synthesis is to reach the highest possible yield of the final product, avoiding the formation of byproducts. For this, the conditions that influence these reactions can be optimized, such as the solvent, catalyst, concentration, temperature, type of reagent and functional groups [2]. In a more effective way than traditional organic synthesis with several stages, MS can form larger structures in a single step. The process allows automation and involves only one step of purification, as it is not necessary to isolate intermediates, thus simplifying the synthesis execution and decreasing the generation of chemical residues [3].

Some MS procedures stand out due to the potential application of the synthesized compounds in the pharmaceutical field. The literature describes, for example, the Biginelli reaction for the formation of dihydropyrimidones [4], the Bucherer-Bergs reaction for the formation of hydantoins [5], the Hantzsch reaction for the formation of dihydropyridines [6] and the Strecker reaction for the formation of amino acids [7].

Hexahydroquinolines (HQs) are interesting carbonic skeletons from a pharmacological point of view. Compounds in this class have attracted attention in recent years because of their significant biological activities and have been described as excellent cardiovascular agents. Several derivatives of this class are effective and promising in the treatment of arterial hypertension [8]. Structurally, these compounds are analogous to NADH coenzymes and have been explored as calcium channel antagonists. In addition, heterocyclic rings are found in a wide variety of bioactive compounds such as bronchodilators, antiatherosclerotic compounds, antitumor compounds, vasodilators, antidiabetic compounds, antimicrobial compounds and hepatoprotective compounds [9–12]. Several drugs from this class have already been commercialized, such as nifedipine, felodipine, amlodipine and nitrendipine [13]. For these reasons, hexahydroquinolines not only draw the atten-

* Corresponding author.
E-mail address: luca@ufla.br (L.M.A. Pinto).

https://doi.org/10.1016/j.molstruc.2021.130391
0022-2860/

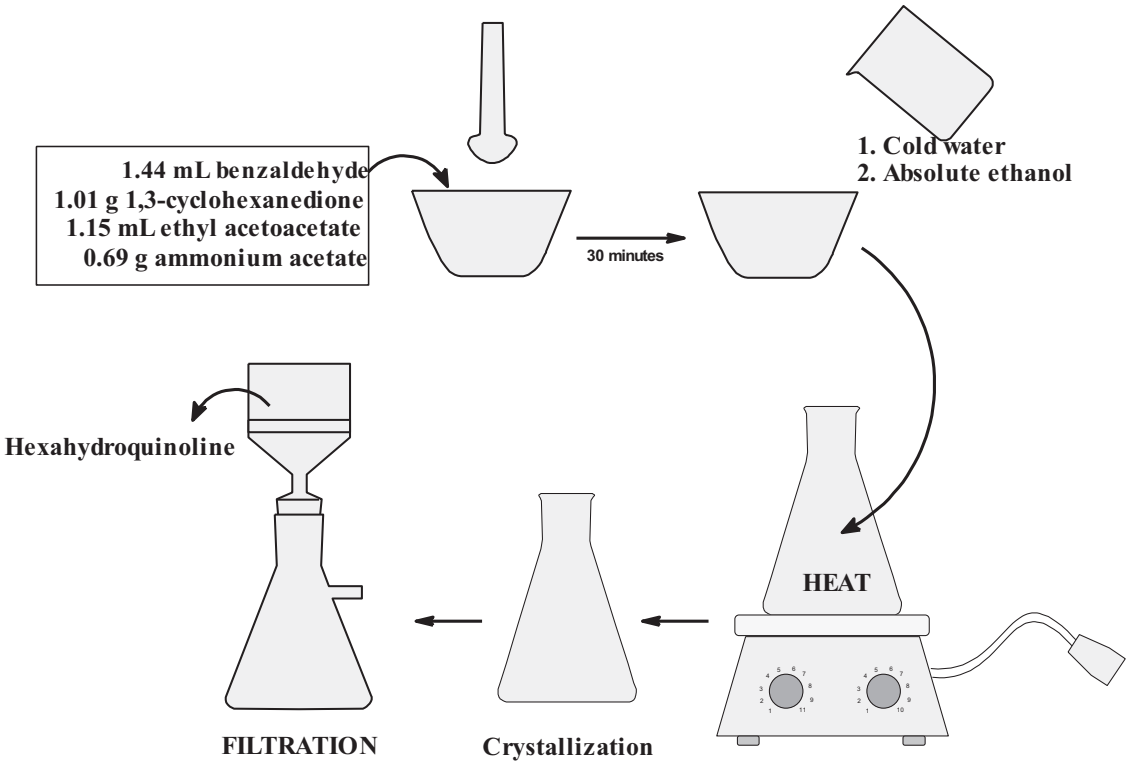

Scheme 1. Description of the steps carried out in the multicomponent synthesis of HQ.

tion of chemists to synthesize them but also represent an interesting research challenge.

Although there are other methods for obtaining HQs, most of them involve the use of solvents, catalysts, heating and long reaction times. Thus, in this work we opted for the methodology that is more in line with the context of green chemistry [14,15].

When analyzing the chemical structure of HQ (Fig. 1-insert), it is possible to notice that one problem that may interfere with the mechanism of action of this compound is its low solubility in water [16]. In addition, these molecules can suffer photodegradation, which can cause loss of therapeutic effect [17]. One way to improve the activity of these substances, in the case of *in vivo* tests, is to increase the solubility in water and consequently the bioavailability. To achieve this goal, the preparation of inclusion complexes with cyclodextrins (CDs) could lead to this increase in solubility, promote a slower release of the compound after administration and prevent possible toxicity. Thus, the objective of this work was to obtain and characterize an HQ compound (ethyl 2-methyl-5-oxo-4-phenyl-1,4,5,6,7,8-hexahydroquinoline-3-carboxylate) using MS. Afterward, an inclusion complex with cyclodextrin was prepared and characterized to test the molecule as a potential medicine.

2. Material and methods

2.1. Multicomponent synthesis and characterization of HQ

The MS is described in the following Scheme 1. To a mortar was added 1.44 mL of benzaldehyde, 1.01 g of 1,3-cyclohexanedione, 1.15 mL of ethyl acetoacetate and 0.69 g of ammonium acetate. The components were macerated for 30 min with a pestle until the mass had the consistency of glue. Then, a small amount of cold water was added to obtain the product, which was transferred to an Erlenmeyer flask. Absolute ethanol was added, and the flask was heated until the solution became translucent [6]. After crystallization, HQ was filtered for further characterization by Fourier transform infrared spectroscopy using a Bruker Alpha II Fourier transform infrared spectrometer and by ^{1}H, ^{13}C and HMQC nuclear magnetic resonance, recorded at 20 °C on a Bruker Ultra-Shield 300 MHz spectrometer using $DMSO_{d6}$ or $CDCl_3$ as the solvent. Chemical shifts (δ) were reported in parts per million (ppm) relative to the residual solvent peak.

2.2. Selection of the cyclodextrin using inclusion kinetics

An experiment was performed to determine the equilibrium rate for the inclusion process and to define which cyclodextrin is the best to prepare the inclusion complex. Two types of cyclodextrins (β- and γ-CD) were used to determine which of them better accommodates the HQ molecule into the cavity. Appropriate amounts of HQ and β- or γ-CD at 1:1 and 1:2 molar ratios were placed in ultrapure water and stirred at 25 °C. A control with plain HQ was also performed using the same conditions. At specific times, aliquots were measured by UV–Vis spectrophotometry at 245 nm until a plateau was reached. Absorbances were normalized in relation to the initial absorbance, and the curves obtained were analyzed using a linear regression of the data: absorbance *vs* time, ln absorbance *vs* time and 1/absorbance *vs* time (zero-, first- and second-order models respectively) to determine the kinetic constant of the process [18–20].

2.3. Evaluation of the inclusion process

2.3.1. Phase solubility isotherm

Increasing amounts of β-CD (0–15 mM) and an excess amount of HQ (5 mM) were placed in appropriate flasks with ultrapure water. The samples were shaken for 24 h at 25 °C and then centrifuged at 14,000 rpm for 20 min. The supernatant was filtered and measured by UV–Vis spectrophotometry at 245 nm. The association constant (K_a) was determined using Eq. (1) proposed by Higuchi and Connors [21], where S_0 is the intrinsic solubility of

HQ.

$$Ka = \frac{slope}{S_0(1 - slope)} \quad (1)$$

The thermodynamic parameter of the standard Gibbs free energy ($\Delta G°$) was also determined using Eq. (2), where S_0 and S_s are the HQ solubility in the absence and presence of β-CD, respectively [20,22,23].

$$\Delta G^0 = -2.303RTlog\left(\frac{S_s}{S_0}\right) \quad (2)$$

2.3.2. Proton nuclear magnetic resonance

$DMSO_{d6}$ solutions of HQ, β-CD and the HQ/β-CD inclusion complex were prepared for ^{1}H NMR experiments recorded at 20 °C in a Bruker Ultra-Shield 300 MHz spectrometer. Chemical shifts (δ) were reported in parts per million (ppm) relative to the residual solvent peak to observe changes after complexation.

2.4. Inclusion complex preparation

2.4.1. Kneading method

Appropriate amounts of HQ and β-CD were weighed to give 1:1 and 1:2 molar ratios. The compounds were kneaded in a mortar with a small amount of absolute ethanol for 30 min. The obtained paste was kept in a desiccator until completely dry.

2.4.2. Lyophilization method

HQ and β-CD were weighed to give 1:1 and 1:2 molar ratios and then solubilized in absolute ethanol and ultrapure water, respectively. The two solutions were then mixed in a round bottom flask and coevaporated to remove all the solvent. After drying, the product was resuspended in 20 mL of ultrapure water, lyophilized, and stored for further use.

2.5. Characterization of the inclusion complexes

2.5.1. Differential scanning calorimetry

Calorimetric assays were performed on a DSC Q200 (TA Instruments). Samples (3 to 5 mg) of HQ, β-CD, and HQ/β-CD inclusion complexes obtained by kneading and lyophilization, as well as physical mixtures at 1:1 and 1:2 molar ratios, were weighed and placed in aluminum pans with a hole. Scans were performed from 30 to 300 °C with a heating rate of 10 °C/min. The atmosphere was N_2 at a flow rate of 50 mL/min.

2.5.2. Near-infrared spectroscopy

The procedure was performed in a NIR-ATR ABB - Model TLA 2000, with the same samples tested in the DSC assays. The following parameters were used in the experiments: a resolution of 8 cm^{-1}, 75 scans min^{-1}, a range from 4000 to 10,000 cm^{-1}, using GRAMS AI 7.0.0 software.

2.5.3. In vitro dissolution assay

Plain HQ and HQ/β-CD inclusion complexes obtained by kneading and lyophilization at 1:1 and 1:2 molar ratios were mixed in appropriate flasks with ultrapure water in triplicate. Samples were shaken for 120 min at 37 °C, and every 5 min an aliquot was withdrawn, filtered, and measured at 245 nm in a UV–Vis spectrophotometer. The volume of the samples was replaced with ultrapure water after each estimation [20,24].

3. Results and discussion

3.1. Characterization of HQ and proposed mechanism of reaction

A pale-yellow powder of HQ was obtained with an 86% yield. Further spectroscopic characterization was performed to confirm the product.

The FTIR spectra of HQ is shown in Fig. 1. The band at 3281 cm^{-1} is related to bending from the secondary N–H amine. Aromatic C–H stretching is observed in the range of 2959–3070 cm^{-1}, and the C=O ketone appears at 1687 cm^{-1}. The signal at 1601 cm^{-1} indicates the presence of a monosubstituted benzene, and the signal at 1471 cm^{-1} indicates the C–C stretching vibrations of the aromatic ring. Peaks in the region of 1225–1056 cm^{-1} are associated with C–CO–O ester vibrations.

Analysis of the ^{1}H NMR spectra obtained using $DMSO_{d6}$ as a solvent (Fig. 2-a) showed a singlet at δ=9.11 ppm relative to the

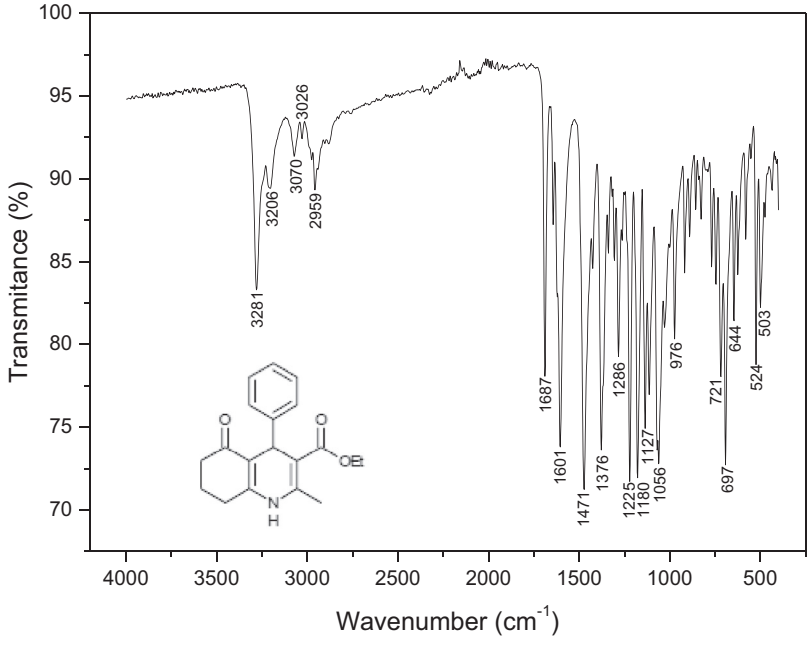

Fig. 1. Fourier transform infrared spectroscopy of HQ obtained in a Bruker, model Alpha II.

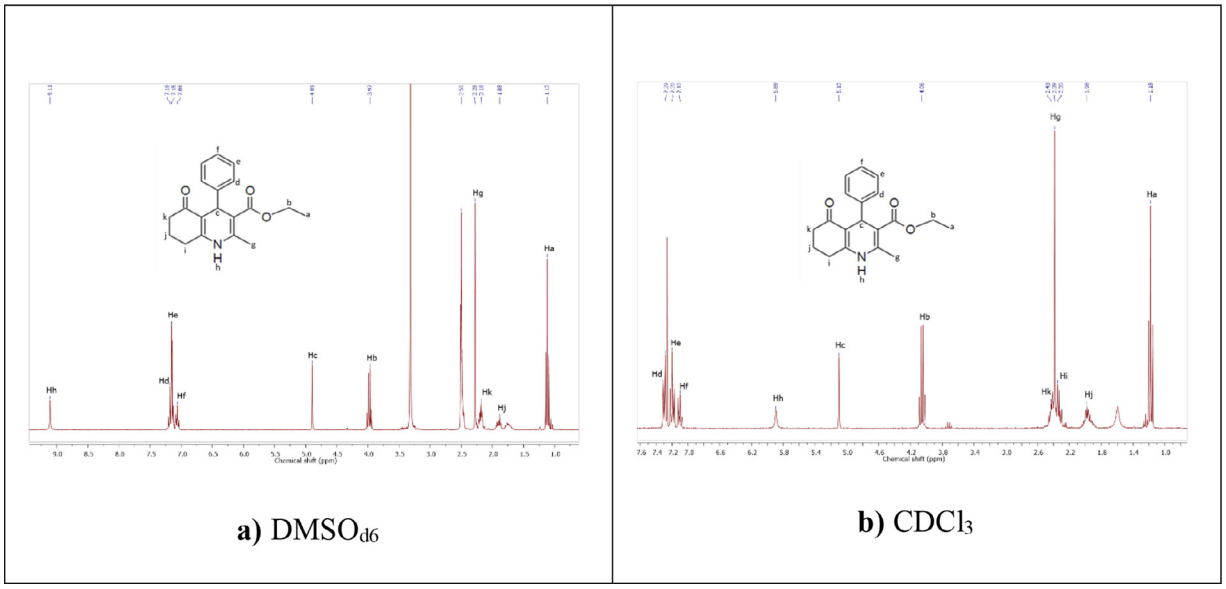

Fig. 2. ^{1}H NMR spectra of HQ in a) $DMSOd_6$ and b) $CDCl_3$ solvent, recorded on a Bruker 300 MHz spectrometer, at 20 °C.

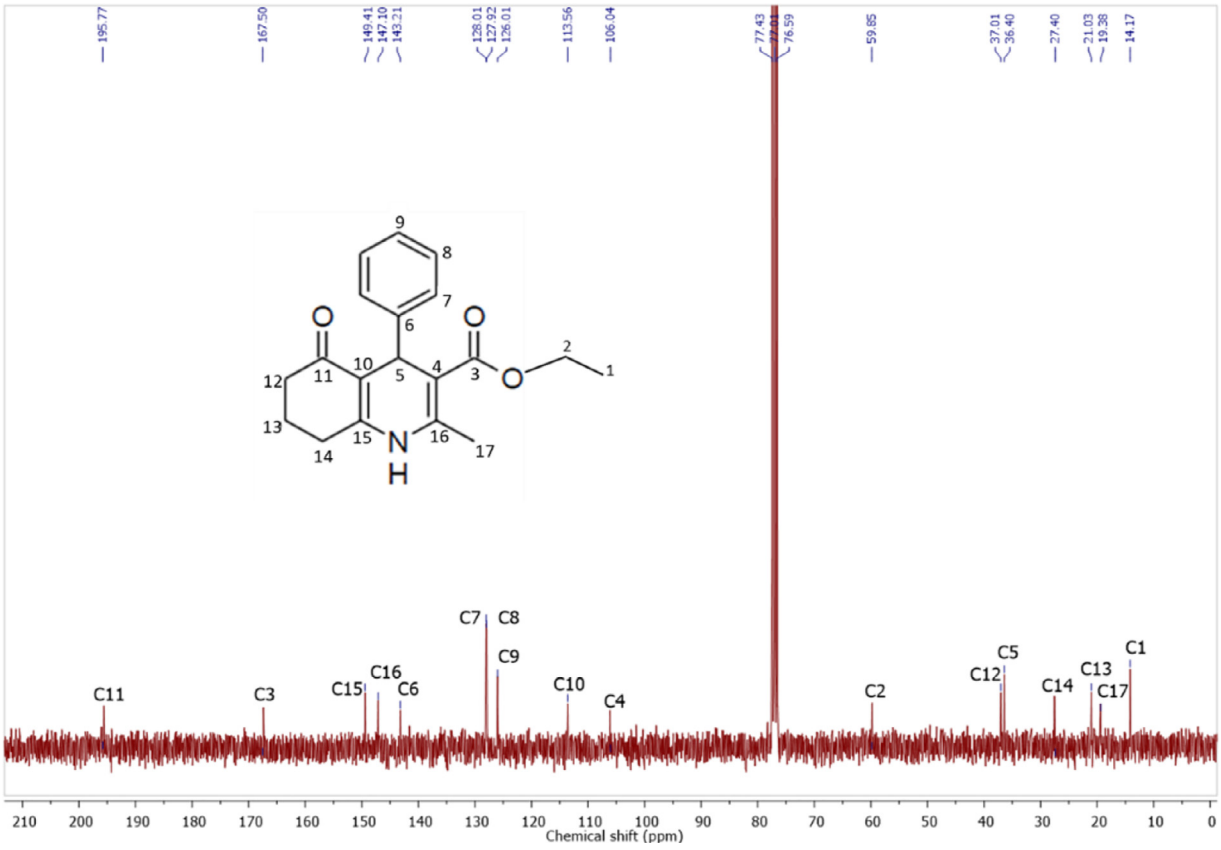

Fig. 3. 75 MHz ^{13}C NMR spectra of HQ in $CDCl_3$ solvent, recorded on a Bruker spectrometer, at 20 °C.

amino proton (Hh). A multiplet in the aromatic region that integrates into five hydrogen atoms indicates an aromatic monosubstituted ring ($\delta \approx 7{,}14$, Hd, He, Hf). Another singlet at $\delta = 4.90$ ppm, which integrates into one proton, is compatible with the chemical shift of the hydrogen in the pyridinic system (Hc). In the aliphatic portion of the molecule, a quartet at $\delta = 3.98$ ppm (Hb) and a triplet at $\delta = 1.12$ ppm (Ha) indicate the presence of an ethyl group. Some multiplets between $\delta = 2.30$ and $\delta = 1.75$ ppm are compatible with the methylene groups (Hj, Hk) from the left ring. The peak assigned to proton Hi is superimposed with the solvent peak. Finally, a singlet was detected at $\delta = 2.28$ ppm, indicating protons from the methyl group linked to the pyridinic ring (Hg). The ^{1}H spectra obtained using $CDCl_3$ as the solvent (Fig. 2-b) is similar to that obtained with $DMSOd_6$, with the exception of the amino proton Hh, which is more deshielded, and the Hi proton, which is no longer superimposed and appears in the same region as the Hj and Hk protons.

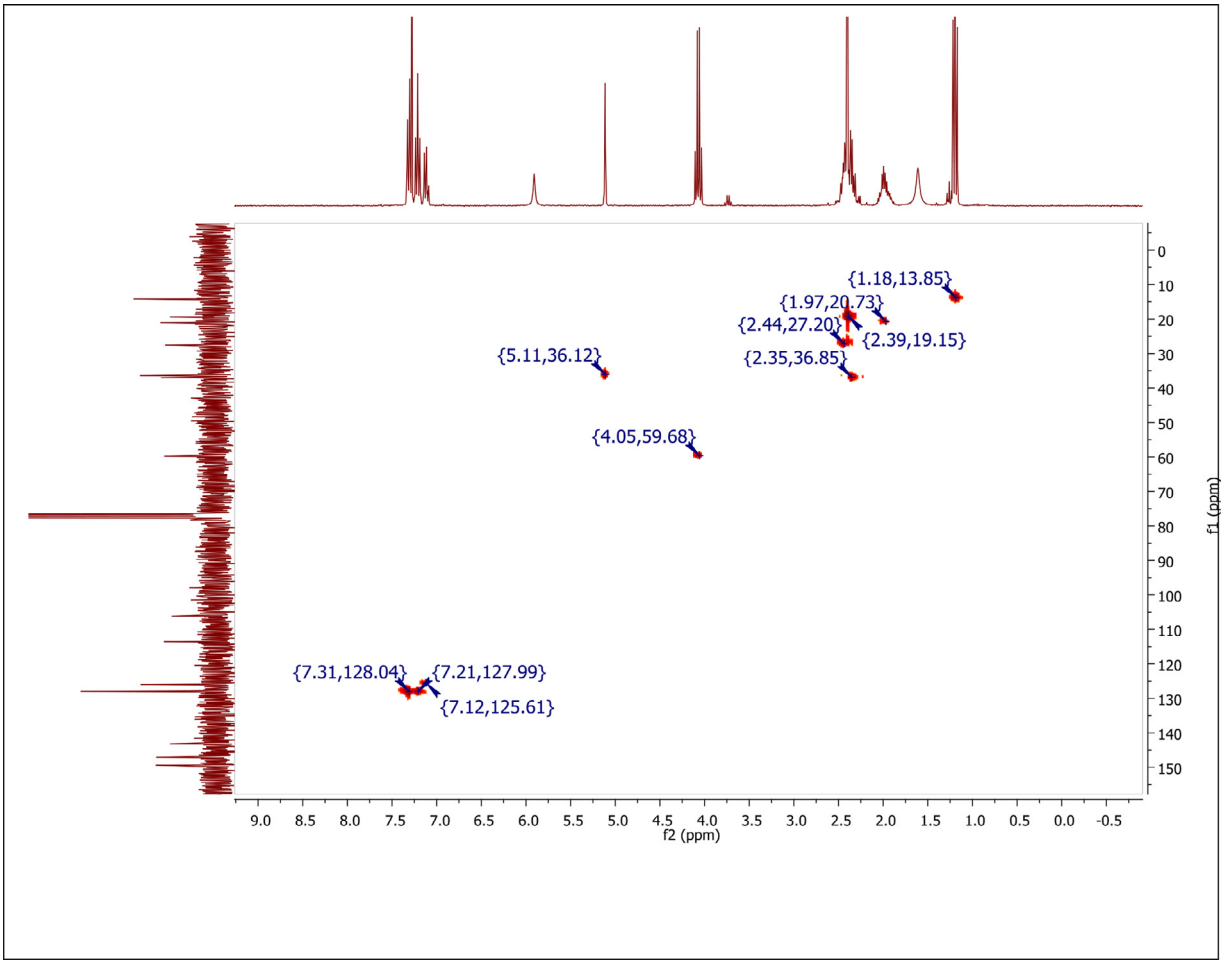

Fig. 4. HMQC-2D correlation of HQ in $CDCl_3$ solvent, recorded on a Bruker 300 MHz spectrometer at 20 °C.

^{13}C NMR spectra (Fig. 3) showed 19 carbon atoms, 12 with ^{2} hybridization and 7 with sp^3 hybridization. The chemical shifts recorded at δ=195.77 and δ=167.50 ppm were related to the carbonyls of the ketone (C11) and ester (C3), respectively. Double bonds of the 1,4-di-hydropiridinic ring appeared at δ=149.41 (C16), δ=147.10 (C15), δ=113.56 (C10) and δ=106.04 ppm (C4). The aromatic carbons showed signals at δ=143.21 (C6), δ=128.01 (C8), δ=127.92 (C7) and δ=126.01 ppm (C9). The ethyl group connected to the ester showed chemical shifts at δ=59.85 (C2) and δ=14.17 ppm (C1). For the methylenic groups, the signals appeared at δ=37.01 (C14), δ=27.40 (C12) and δ=21.03 ppm (C13). C5 was observed at δ=36.40 ppm, and the resonance at δ=19.38 ppm was consistent with the methyl group of C17.

The HMQC spectra showed the cross peaks (Hd-C7), (Hc-C5), (Hb-C2), (Hg-C17), (Ha-C1), and (Hj-C13), confirming the assignment of the synthetized molecule (Fig. 4).

Several reaction paths have already been examined for this type of reaction. A reasonable proposal is that initially, there is an aldolic condensation between 1,3-cyclohexanedione and benzaldehyde to form a Michael's acceptor as an intermediate. This intermediate should react with ethyl acetoacetate through a conjugated addition (Michael addition). One of the ketone carbonyls must react with ammonia present in the reaction medium to form an imine, which undergoes enamine tautomerism to promote an internal nucleophilic attack on another ketone carbonyl, closing the 1,4-dihydropyridine ring. The mechanism of the reaction is detailed in Fig. 5.

3.2. Selection of the cyclodextrin using inclusion kinetics

The inclusion of a guest molecule inside the cyclodextrin cavity can lead to changes in the spectroscopic characteristics of the molecule to be included. A decrease in the polarity of the environment after complexation may reflect, in most cases, an increase in the UV–Vis absorbance of the guest, and interactions between the guest and host occur due to the polarity and steric effects of the system [18,19].

In this study, the tested solutions reached equilibrium in approximately 60 min (Fig. 6) after a linear increase in the absorbance, showing that a relatively short time is needed to obtain inclusion complexes. No batho- or hypsochromic shifts were observed in any of the tested samples during the experiment time, and in relation to the hyperchromic effect, we observed the following order: β-CD 1:2 > β-CD 1:1 > γ-CD 1:2 > plain HQ > γ-CD 1:1. Thus, the solution containing β-CD induced the greatest increase in absorbance and proved to be the best at incorporating the HQ molecule and was therefore used to prepare the inclusion complexes for this work.

After analyzing the kinetic profile with β-CD, zero-order complexation kinetics were determined, with R^2 = 0.98683 and 0.99509 at 1:1 and 1:2 stoichiometry, respectively. The kinetic constants (k) were calculated to be $7.74 \times 10^{-2} \pm 2.48 \times 10^{-3}$ h^{-1} (1:1) and $9.73 \times 10^{-2} \pm 1.9 \times 10^{-3}$ h^{-1} (1:2), in accordance with values found previously in the literature for apolar molecules such as praziquantel [18,19] and dibenzalacetone [20]. The result

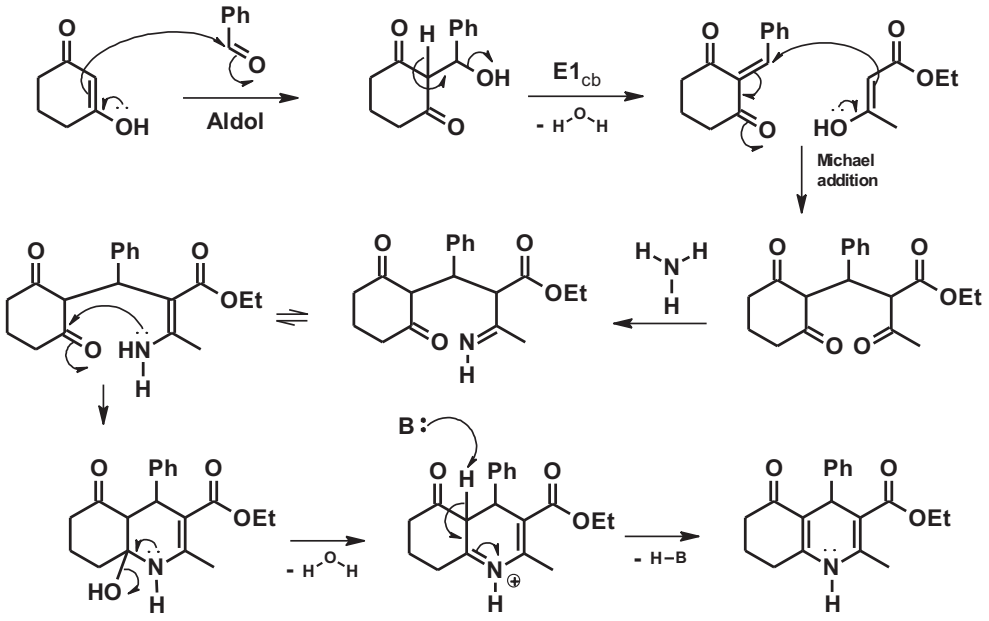

Fig. 5. Proposed mechanism of reaction for the multicomponent synthesis of HQ.

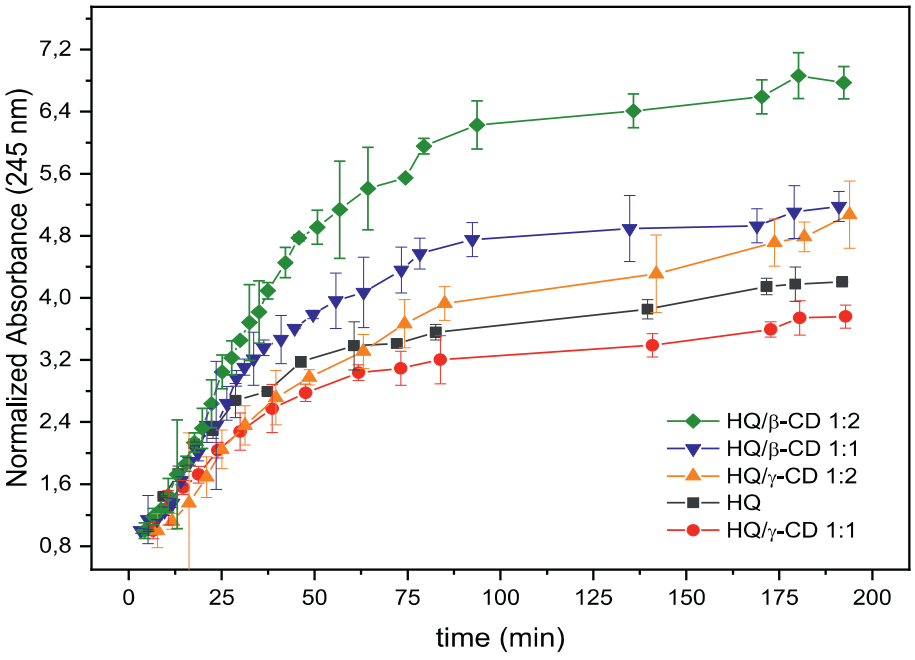

Fig. 6. Inclusion kinetics of HQ with β-CD and γ-CD at 1:1 and 1:2 stoichiometries at 25 °C.

suggests that in both molar ratios, the formation of the inclusion complex occurs, with the 1:2 molar ratio being the most likely to happen, as corroborated by other analyses shown hereafter.

3.3. Evaluation of the inclusion process

3.3.1. Phase solubility isotherm

Analysis of the phase solubility allows the evaluation of the affinity of the guest molecule for the cavity of cyclodextrin in water. The solubility of the HQ molecule increased 3.5-fold in the presence of β-CD up to 15 mM, giving an A_L profile (Fig. 7) according to the classification of Higuchi and Connors [21]. The association constant K_a was determined to be 170.3 M^{-1}, which is considered a suitable value to improve the solubility of hydrophobic molecules. Some reports about poorly soluble compounds describe an increase of 3.4-fold for atrazine, with Ka = 130.68 M^{-1} [25]; for benzocaine, the solubility increased 3 times, with Ka = 229.8 M^{-1} [26], and for praziquantel, the Ka was 140.8 M^{-1}, with a 5.5-fold increase in aqueous solubility [19].

The standard Gibbs free energy ($\Delta G°$) was used to analyze the tendency of the guest molecule to interact inside the carrier system, indicating whether this condition increases the solubilization.

The values obtained for HQ were negative and increased at all concentrations of β-CD (Table 1), indicating that the process to transfer the molecules toward the cavity is spontaneous and is favored as the concentration of β-CD increases.

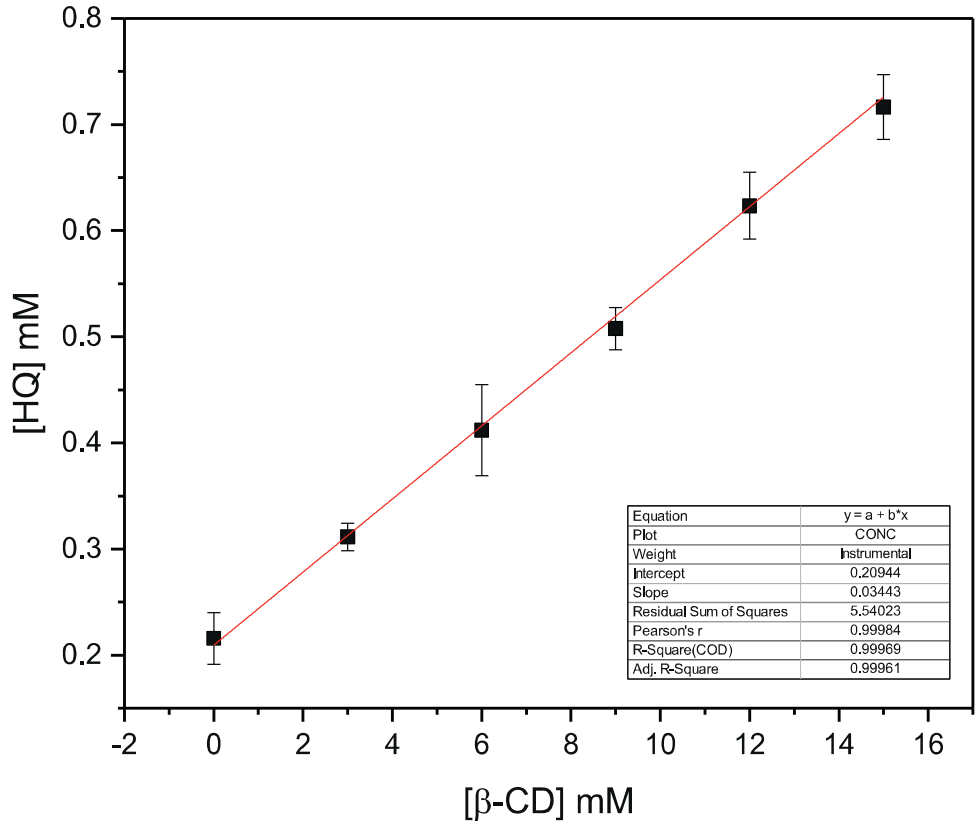

Fig. 7. Phase solubility isotherm for HQ at increasing concentrations of β-CD in water at 25 °C.

Table 1
Standard Gibbs free energy ($\Delta G°$) for solubilization of HQ in aqueous solution of β-CD.

[β-CD] mM	$\Delta G°$ (KJ mol^{-1})
3	−0.994
6	−1.702
9	−2.251
12	−2.701
15	−3.082

3.3.2. Nuclear magnetic resonance

^{1}H NMR spectroscopy was employed to investigate the interaction of the HQ molecule with β-CD and suggest how the interaction occurs. Changes in the chemical shift after inclusion are a sign that the proton is under the influence of other protons nearby and can help determine a possible geometry of the inclusion. On the other hand, sometimes changes are not sufficient to be measured, and additional experiments are needed to elucidate the complexation. In the case of HQ, the cyclohexanone (Hj) and aromatic ring (Hf) likely interact with the head of β-CD, as H1, OH3 and H2 were the most affected protons from the cyclodextrin (Table 2). Further studies using 2D ROESY could help to clarify the interaction between the molecules, tracing the spatial interaction between the host and guest.

3.4. Characterization of the inclusion complexes

3.4.1. DSC

For plain β-CD, an endothermic peak at 112.27 °C was observed, which corresponds to the loss of water molecules from the cavity (Fig. 8) and is in agreement with other data [27,28]. On the other hand, the HQ molecule showed a sharp peak at 262.31 °C, related to its melting temperature [16].

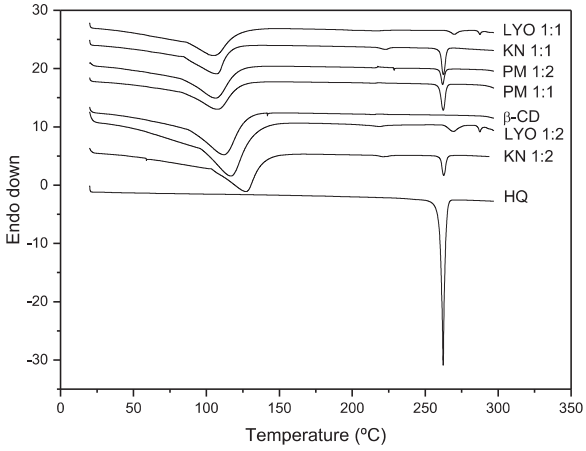

Fig. 8. DSC thermograms of HQ, β-CD, HQ/β-CD inclusion complexes obtained by kneading (KN) and lyophilization (LYO) methods and physical mixtures (PM) at 1:1 and 1:2 molar ratios.

For the inclusion complexes LYO and KN at a 1:1 molar ratio, a decrease in the transition temperature of approximately 10 °C occurred because water molecules left the cavity earlier to accommodate the HQ structure. At a 1:2 molar ratio, there was proportionally more β-CD than HQ, and probably not all the water molecules were displaced by HQ, which can be determined from the transition peak at higher temperatures. The PM at both stoichiometries had similar behavior, with a decrease in the transition peak related to β-CD.

Table 2
^{1}H NMR chemical shifts of β-CD and HQ protons in $DMSO_{d6}$ before and after complexation.

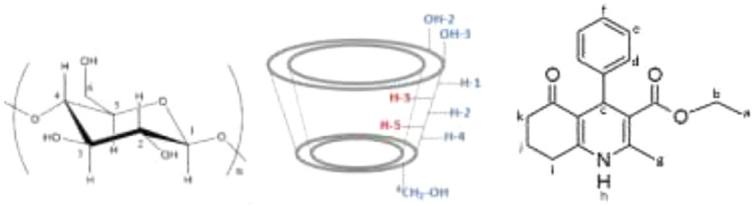

Assignment	β-CD (ppm)	HQ (ppm)	HQ/β-CD (ppm)	$\Delta\delta$ (ppm)
H2	**nd**		**3.29**	**0.04**
H4	3.30		3.28	0.02
H5	3.63		3.61	0.02
H3	3.66		3.67	0.01
H6	3.55		3.55	0
OH6	4.44		4.43	0.01
H1	**4.83**		**4.88**	**0.05**
OH2	5.70		5.70	0
OH3	**5.65**		**5.70**	**0.05**
Ha		1.12	1.10	0.02
Hb		3.98	3.97	0.01
Hc		4.89	4.92	0.03
Hd		7.19	7.18	0.01
He		7.15	7.14	0.01
Hf		**7.07**	**7.12**	**0.05**
Hg		2.28	2.27	0.01
Hh		9.11	9.11	0
Hi		nd	–	–
Hj		**1.88**	**2.08**	**0.20**
Hk		2.21	2.18	0.03

nd: not determined due to peak overlap.

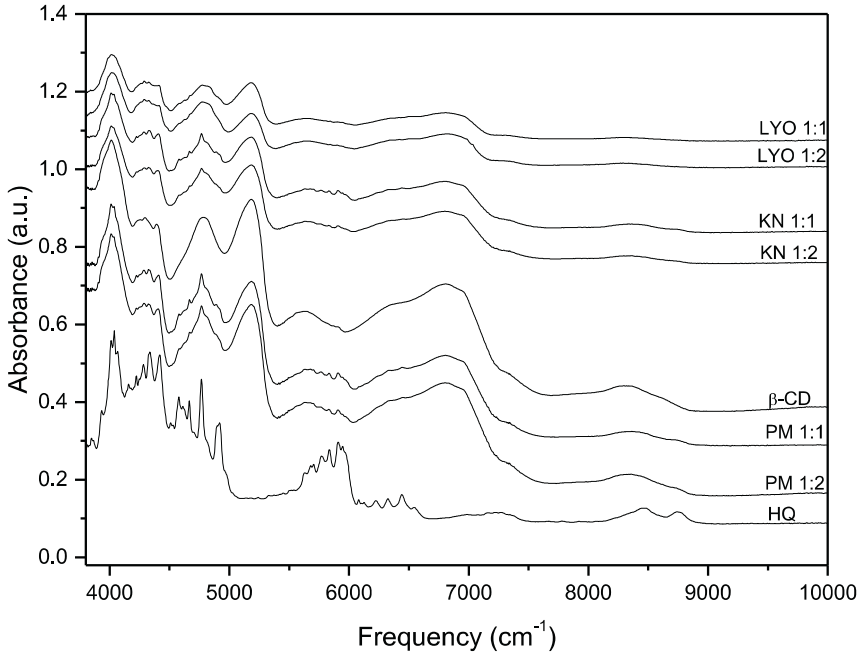

Fig. 9. NIR spectra of HQ, β-CD, HQ/β-CD inclusion complexes obtained by kneading (KN) and lyophilization (LYO) methods and physical mixtures (PM) at 1:1 and 1:2 molar ratios.

Upon analyzing the transition peak of HQ, it is observed that KN and PM at 1:1 and 1:2 stoichiometries presented Tmax values at the same temperature as HQ alone. The intensity decreased but was similar in all the samples. These results demonstrate that these methods were not useful for complexing the HQ molecule inside β-CD. Otherwise, LYO at 1:1 and 1:2 molar ratios shifted Tmax to higher temperatures with a smaller enthalpy, probably due to the shielding of HQ inside the β-CD cavity, which would cause the molecule to shift its melting temperature to higher values. They also exhibited another peak at higher temperatures that indicate that some residual HQ is released from the cavity.

3.4.2. NIR

NIR spectra were collected in diffuse reflectance mode (Fig. 9). HQ gave rise to sharp bands in the overtone region at 6000 cm^{-1} and 6500 cm^{-1} assigned to the C–H and N–H vibrations modes, respectively, while β-CD gave rise to wide bands from the hydroxyl groups [20].

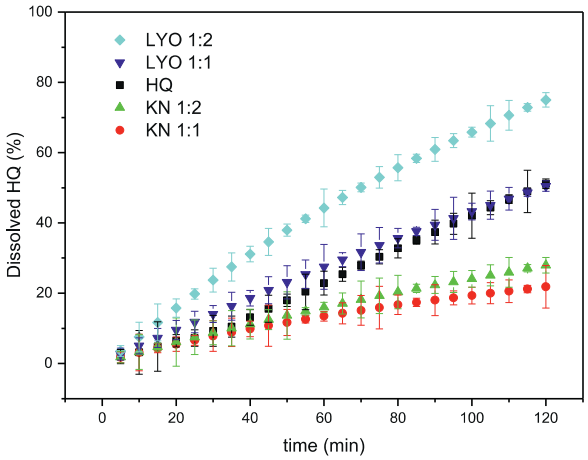

Fig. 10. Dissolution profiles of HQ and HQ/β-CD inclusion complexes obtained by kneading (KN) and lyophilization (LYO) methods at 1:1 and 1:2 molar ratios.

Table 3
Dissolution data for HQ and HQ/β-CD inclusion complexes in water.

Samples	DP_{30} (%)	T_{50} (min)
LYO 1:2	23.6	70.0
LYO 1:1	14.1	117.5
HQ	9.4	117.5
KN 1:2	8.5	> 120.0
KN 1:1	7.6	> 120.0

The spectra of the complexes obtained by KN and LYO were more similar to that of β-CD alone, but LYO lost the characteristic bands of HQ at 8500–8700 cm^{-1}, indicating that complexation was more efficient in this method.

The spectra of PM, at both molar ratios, is superimposed with those of HQ and β-CD alone, indicating that a weak interaction may occur in this preparation.

3.4.3. In vitro dissolution assay

Dissolution studies of HQ and systems containing β-CD are shown in Fig. 10. After 120 min of shaking, the sample with the inclusion complex obtained by lyophilization at a 1:2 molar ratio had an improved rate of HQ dissolution. The other samples decreased (KN 1:1 and 1:2) or maintained (LYO 1:1) the dissolution profile of HQ alone at the end of the experiment.

The % of drug dissolved within 30 min (DP_{30}) and the time to dissolve 50% of the drug (T_{50}) were determined and are summarized in Table 3. The DP_{30} increased for the inclusion complexes obtained by LYO and decreased for those obtained by KN, confirming that the lyophilization method is more suitable to prepare the complex. Some of the mechanisms that could explain the increase in the dissolution rate are the reduction in crystallite size, the effect of solubilization of the CD and conversion of the drug to an amorphous state (Patel & Patel, 2010). LYO 1:2 was the only sample that had a considerable decrease in the T_{50} parameter compared to HQ alone. Therefore, LYO at a 1:2 stoichiometry is considered the best formulation to improve the solubility of the HQ drug, even though the time was not enough to reach the plateau at 100% dissolution.

4. Conclusions

The multicomponent synthesis presented a good yield, demonstrating that it is a fast and environmentally safe alternative for obtaining the HQ molecule and can be used to obtain other analogous molecules of biological interest. The proposed mechanism of the reaction involved a Michael addition reaction. The cyclodextrin selected to prepare the inclusion complexes was β-CD, that increased its aqueous solubility, which may reflect a greater stability and activity of the molecule. Lyophilization at a 1:2 molar ratio was the best procedure to prepare the inclusion complexes, which can be submitted to *in vitro* assays to demonstrate whether HQ shows an improvement in its biological properties. Furthermore, inclusion in the cavity of β-CD can favor groups of the HQ molecule to interact more appropriately in their place of action, leading to a better response of the organism.

Declaration of Competing Interest

The authors declare that they have no known competing financial interests or personal relationships that could have appeared to influence the work reported in this paper.

CRediT authorship contribution statement

Luciana Matos Alves Pinto: Conceptualization, Methodology, Formal analysis, Investigation, Writing - original draft, Writing - review & editing. **Oluwatomide Adeoye:** Methodology, Formal analysis, Investigation, Writing - review & editing. **Sérgio Scherrer Thomasi:** Methodology, Resources, Formal analysis, Writing - review & editing. **Helena Cabral-Marques:** Conceptualization, Resources, Writing - original draft, Supervision, Funding acquisition.

Acknowledgments

This work was supported by the Research Institute for Medicines (iMed-ULisboa) through FCT/MCTES (UID/DTP/04138/2019), Central de Análise e Prospecção Química (CAPQ), Fundação de Amparo à Pesquisa de Minas Gerais (FAPEMIG), Coordenação de Aperfeiçoamento de Pessoal de Nível Superior (CAPES), and Conselho Nacional de Desenvolvimento Científico e Tecnológico (CNPq).

References

[1] M.V. Marques, T.B. Bisol, M.M. Sá, Reações multicomponentes de Biginelli e de Mannich nas aulas de química orgânica experimental: uma abordagem didática de conceitos da química verde, Quím. Nova 35 (8) (2012) 1696–1699, doi:10.1590/s0100-40422012000800034.
[2] R.C. Cioc, E. Ruijter, R.V.A. Orru, Multicomponent reactions: advanced tools for sustainable organic synthesis, Green Chem. 16 (6) (2014) 2958–2975, doi:10.1039/c4gc00013g.
[3] N. Elders, D. van der Born, L.J.D. Hendrickx, B.J.J. Timmer, A. Krause, E. Janssen, F.J.J. de Kanter, E. Ruijter, R.V.A. Orru, The efficient one-pot reaction of up to eight components by the union of multicomponent reactions, Angew. Chemie 121 (32) (2009) 5970–5973, doi:10.1002/ange.200902683.
[4] S.R. Roy, P.S. Jadhavar, K. Seth, K.K. Sharma, A.K. Chakraborti, Organocatalytic application of ionic liquids: [bmim][MeSO4] as a recyclable organocatalyst in the multicomponent reaction for the preparation of dihydropyrimidinones and -thiones, Synthesis 14 (2011) 2261–2267, doi:10.1055/s-0030-1260067.
[5] J.L. Monteiro, B. Pieber, A.G. Corrêa, C.O. Kappe, Continuous synthesis of hydantoins: intensifying the Bucherer-Bergs reaction, Synlett 27 (1) (2016) 83–87, doi:10.1055/s-0035-1560317.
[6] A. Kumar, R.A. Maurya, Efficient synthesis of Hantzsch esters and polyhydroquinoline derivatives in aqueous micelles, Synlett 2008 (06) (2008) 883–885, doi:10.1055/s-2008-1042908.
[7] J.-.B. Gualtierotti, X. Schumacher, Q. Wang, J. Zhu, Synthesis of iminonitriles by oxone-TBAB-mediated one-pot oxidative three-component Strecker reaction, Synthesis 2 (2013), doi:10.1055/s-0032-1316980.
[8] F.R. Bühler, W. Kiowski, Age and antihypertensive response to calcium antagonists, J. Hypertens. 5 (4) (1987) S111–S114, doi:10.1097/00004872-198712004-00017.
[9] P.P. Mager, R.A. Coburn, A.J. Solo, D.J. Triggle, H. Rothe, QSAR, diagnostic statistics and molecular modelling of 1,4-dihydropyridine calcium antagonists: a difficult road ahead, Drug Des. Discov. 8 (4) (1992) 273–289.
[10] O. Özbek, N.C. Usta, M.B. Gürdere, O.N. Aslan, Y. Budak, M. Ceylan, Synthesis and antibacterial screening of novel 2-(4-(aryl) thiazol-2-yl)-3a,4,7,7a-tetrahydro-1H-4,7-ethanoisoindole-1,3(2H)-dione derivatives, Phosphorus, Sulfur, Silicon Relat. Elem. 192 (10) (2017) 1153–1157 10.1080/10426507.2017.1354209, doi:10.1080/10426507.2017.1354209.

[11] H. Gezegen, M.B. Gürdere, A. Dinçer, O. Özbek, Ü.M. Koçyiğit, P. Taslimi, B. Tüzün, Y. Budak, M. Ceylan, Synthesis, molecular docking, and biological activities of new cyanopyridine derivatives containing phenylurea, Arch. Pharm. (2020) e2000334 n/a (n/a), doi:10.1002/ardp.202000334.
[12] O. Özbek, M.B. Gürdere, Synthesis and anticancer properties of 2-aminothiazole derivatives, Phosphorus, Sulfur, Silicon Relat. Elem. (2021) 1–11, doi:10.1080/10426507.2020.1871347.
[13] J.P. Wan, Y. Liu, Recent advances in new multicomponent synthesis of structurally diversified 1,4-dihydropyridines, RSC Adv. 2 (26) (2012) 9763–9777, doi:10.1039/c2ra21406g.
[14] D. Azarifar, R. Asadpoor, O. Badalkhani, M. Jaymand, E. Tavakoli, M. Bazouleh, Sulfamic-acid-functionalized $Fe_{3-x}Ti_xO_4$ nanoparticles as novel magnetic catalyst for the synthesis of hexahydroquinolines under solvent-free condition, Chemistry Select 3 (48) (2018) 13722–13728, doi:10.1002/slct.201802505.
[15] S. Kalhor, M. Yarie, M. Rezaeivala, M.A. Zolfigol, Novel magnetic nanoparticles with morpholine tags as multirole catalyst for synthesis of hexahydroquinolines and 2-amino-4,6-diphenylnicotinonitriles through vinylogous anomeric-based oxidation, Res. Chem. Intermed. 45 (6) (2019) 3453–3480, doi:10.1007/s11164-019-03802-7.
[16] https://scifinder.cas.org (acessed in January, 2021)
[17] W. Maafi, M. Maafi, Modelling Nifedipine photodegradation, photostability and actinometric properties, Int. J. Pharm. 456 (1) (2013) 153–164, doi:10.1016/j.ijpharm.2013.07.075.
[18] I.S. Chaves, S.G. Rodrigues, N.F.S. Melo, M.B. de Jesus, L.F. Fraceto, E. de Paula, L.M.A. Pinto, Alternativas para o tratamento da esquistossomose: caracterização físico-química do complexo de inclusão entre praziquantel e hidroxipropil-β-ciclodextrina, Lat. Am. J. Pharm. 29 (7) (2010) 1067–1074.
[19] S.G. Rodrigues, I.S. Chaves, N.F.S. Melo, M.B. de Jesus, L.F. Fraceto, S.A. Fernandes, E. de Paula, M.P. Freitas, L.M.A. Pinto, Computational analysis and physico-chemical characterization of an inclusion compound between praziquantel and methyl-β-cyclodextrin for use as an alternative in the treatment of schistosomiasis, J. Incl. Phenom. Macrocycl. Chem. 70 (1–2) (2011) 19–28, doi:10.1007/s10847-010-9852-y.
[20] L.M.A. Pinto, O. Adeoye, S.S. Thomasi, A.P. Francisco, M.C. Carvalheiro, H. Cabral-Marques, Preparation and characterization of a synthetic curcumin analog inclusion complex and preliminary evaluation of *in vitro* antileishmanial activity, Int. J. Pharm. 589 (April) (2020) 119764, doi:10.1016/j.ijpharm.2020.119764.
[21] T. Higuchi, K.A. Connors, Phase-solubility techniques, Adv. Anal. Chem. Instrum. 4 (1965) 117–121.
[22] R. Patel, M. Patel, Solid-state characterization and *in vitro* dissolution behavior of lorazepam:hydroxypropyl-β-cyclodextrin inclusion complex, Drug Disc. Therap. 4 (6) (2010) 442–452.
[23] V.R. Yadav, S. Suresh, K. Devi, S. Yadav, Effect of cyclodextrin complexation of curcumin on its solubility and antiangiogenic and anti-inflammatory activity in rat colitis model, AAPS PharmSciTech 10 (3) (2009) 752–762, doi:10.1208/s12249-009-9264-8.
[24] A.A. Haroun, N.R. El-Halawany, Encapsulation of bovine serum albumin within β-cyclodextrin/gelatin-based polymeric hydrogel for controlled protein drug release, IRBM 31 (4) (2010) 234–241, doi:10.1016/j.irbm.2010.02.001.
[25] L.B. Carvalho, L.M.A. Pinto, Formation of inclusion complexes and controlled release of atrazine using free or silica-anchored β-cyclodextrin, J. Incl. Phenom. Macrocycl. Chem. 74 (1–4) (2012) 375–381, doi:10.1007/s10847-012-0125-9.
[26] L.H. Torres, M.Z. Carvalho, P.S. Melo, E. de Paula, A.A. Saczk, L.M.A Pinto, Characterization and cytotoxicity of a benzocaine inclusion complex, J. Incl. Phenom. Macrocycl. Chem. 91 (1–2) (2018) 9–15, doi:10.1007/s10847-018-0791-3.
[27] L.N.S.B. Martins, A.F.A. Venceslau, L.B. Carvalho, C. Jaime, M.G. Cardoso, L.M.A. Pinto, Inclusion complex of *Callistemon viminalis* essential oil prepared by kneading, J. Incl. Phenom. Macrocycl. Chem. (2020), doi:10.1007/s10847-020-00989-w.
[28] L.B. Carvalho, K.K. Burusco, C. Jaime, T. Venâncio, A.F.S. Carvalho, L.D.S. Murgas, L.M.A. Pinto, M.A. de, Complexes between methyltestosterone and β-cyclodextrin for application in aquaculture production, Carbohydr. Polym. 179 (June 2017) (2018) 386–393, doi:10.1016/j.carbpol.2017.09.023.